Molecular Biology of the Cell
Vol. 7, 155–172, January 1996

The Paramyxovirus Simian Virus 5 Hemagglutinin-Neuraminidase Glycoprotein, but not the Fusion Glycoprotein, Is Internalized Via Coated Pits and Enters the Endocytic Pathway

George P. Leser,* Karen J. Ector,* and Robert A. Lamb*†‡

*Department of Biochemistry, Molecular Biology and Cell Biology, and †Howard Hughes Medical Institute, Northwestern University, Evanston, Illinois 60208-3500

Submitted January 17, 1995; Accepted October 2, 1995
Monitoring Editor: Mary-Jane Gething

The hemagglutinin-neuraminidase (HN) and fusion (F) glycoproteins of the paramyxovirus simian virus 5 (SV5) are expressed on the surface of virus-infected cells. Although the F protein was found to be expressed stably, the HN protein was internalized from the plasma membrane. HN protein lacks known internalization signals in its cytoplasmic domain that are common to many integral membrane proteins that are internalized via clathrin-coated pits. Thus, the cellular pathway of HN protein internalization was examined. Biochemical analysis indicated that HN was lost from the cell surface with a $t_{1/2}$ of ~45–50 min and turned over with a $t_{1/2}$ of ~2 h. Immunofluorescent analysis showed internalized SV5 HN in vesicle-like structures in a juxtanuclear pattern coincident with the localization of ovalbumin. In contrast the SV5 F glycoprotein and the HN glycoprotein of the highly related parainfluenza virus 3 (hPIV-3) were found only on the cell surface. Immunogold staining of HN on the surface of SV5-infected CV-1 cells and examination using electron microscopy, showed heavy surface labeling that gradually decreased with time. Concomitantly, gold particles were detected in the endosomal system and with increasing time, gold-labeled structures having the morphology of lysosomes were observed. On the plasma membrane ~5% of the gold-labeled HN was found in coated pits. The inhibition of the pinching-off of coated pits from the plasma membrane by cytosol acidification significantly reduced HN internalization. Internalized HN was co-localized with gold-conjugated transferrin, a marker for the early endosomal compartments, and with gold-conjugated bovine serum albumin, a marker for late endosomal compartments. Taken together, these data strongly suggest that the HN glycoprotein is internalized via clathrin-coated pits and delivered to the endocytic pathway.

INTRODUCTION

Numerous ligands bind to plasma membrane receptors and are taken up by the living cell. Commonly, endocytosis is mediated by clathrin-coated pits in which receptors collect in these specialized regions of the plasma membrane and are internalized. A general feature for efficient (rapid) internalization through coated pits is the presence of a tyrosine in the cytoplasmic tail of the receptor in the consensus sequence NPXY or YXRF (Chen *et al.*, 1990; Collawn *et al.*, 1990; reviewed in Trowbridge *et al.*, 1993). This necessity for a tyrosine was first shown for human low density lipoprotein receptor (LDL) (Lehrman *et al.*, 1985; Davis *et al.*, 1986, 1987) and has now been found for many other receptors including transferrin receptor (Alvarez

‡ Corresponding author: Department of Biochemistry, Molecular Biology and Cell Biology, Northwestern University, 2153 North Campus Drive, Evanston, IL 60208-3500.

et al., 1990; Jing *et al.*, 1990; McGraw and Maxfield, 1990), the polymeric Ig receptor (Breitfeld *et al.*, 1990), the 275-kDa mannose-6-phosphate receptor (Lobel *et al.*, 1989), and lysosomal acid phosphatase, in which the internalization signal is PGYRHV (Lehmann *et al.*, 1992). The recognition of receptors is believed to be mediated by the binding of cytoplasmic tails to adaptins, components of the clathrin-coated pit assembly (Pearse, 1988; Glickman *et al.*, 1989). The tyrosine residue may constitute part of the recognition signal for adaptin binding and it may also be a determinant of structure necessary for adaptin recognition (Bansal and Gierasch, 1991).

Not all proteins are believed to enter the cellular endocytic pathway via coated pits. Caveolae, invaginations of the plasma membrane that are smaller in size than coated pits and appear to lack a dense coat when observed in the electron microscope, are believed by some to be dynamic structures that provide the means of entry for some proteins (Montesano *et al.*, 1982; van Deurs *et al.*, 1993b; Parton *et al.*, 1994), but there is no clear consensus regarding their role in the endocytic process (Watts and Marsh, 1992). There have been reports that glycolipid-anchored proteins such as the folate receptor and a modified CD4 molecule (Rothberg *et al.*, 1990; Keller *et al.*, 1992) concentrate in caveolae and it has been suggested that glycolipid-anchored proteins may lack the means to interact with components of the coated pit. However, it has been reported recently that the glycolipid-anchored prion protein enters the endocytic pathway via clathrin-coated pits in a cell line lacking caveolae (Shyng *et al.*, 1994; Gorodinsky and Harris, 1995), which suggests that alternative internalization signals for clathrin-mediated entry may exist. Although not demonstrating that the glucose transporter GLUT 4 resides in caveolae, recent work by Scherer *et al.* (1994) suggests that caveolae are at least involved in the transport of GLUT 4 in adipocytes. In addition, cholecystokinin, a G-protein coupled receptor, is internalized upon agonist binding via both clathrin-coated pits and caveolae (Roettger *et al.*, 1995). Fluid-phase endocytosis or pinocytosis mediated by membrane ruffling is another means by which solutes (and perhaps surface molecules) can be taken up by a cell (Bar-Sagi and Feramisco, 1986; Hubbard, 1989; West *et al.*, 1989; Racoosin and Swanson, 1992) although this pathway is believed to be largely nonspecific and information on its importance to the endocytic pathway is lacking.

Viral envelope glycoproteins have proven to be useful models for the study of the trafficking of cellular proteins (Matlin *et al.*, 1983; Roth *et al.*, 1986; Ng *et al.*, 1989; reviewed in Doms *et al.*, 1993; Hobman *et al.*, 1993; Balch *et al.*, 1994; Krijnse-Locker *et al.*, 1994). For studying internalization signals, for example, an altered influenza virus hemagglutinin containing a tyrosine substitution in the cytoplasmic tail is endocytosed via clathrin-coated pits whereas the parental molecule remains at the cell surface (Lazarovits and Roth, 1988; Ktistakis *et al.*, 1990). In cells infected with the paramyxovirus simian virus 5 (SV5), two virally encoded integral membrane glycoproteins, hemagglutinin-neuraminidase (HN) and the fusion protein (F), are synthesized and transported through the exocytic pathway to the plasma membrane. HN is a type II integral membrane protein with a C-terminal ectodomain, whereas conversely F is a type I glycoprotein possessing an N-terminal ectodomain (Paterson *et al.*, 1984; Hiebert *et al.*, 1985; Hiebert and Lamb, 1988). Both proteins are incorporated into the envelopes of budding viruses. HN mediates binding of the virus to cell surface molecules containing sialic acid and it also possesses a neuraminidase activity that probably prevents the aggregation of progeny virus. The F protein mediates the pH-independent fusion of virus with the cell plasma membrane. In an earlier study of the intracellular maturation and transport of SV5 HN glycoprotein we observed that HN was turned over from the surface of infected cells and degraded, whereas F accumulated stably on the plasma membrane (Ng *et al.*, 1989). SV5 HN has a 17-residue cytoplasmic tail (NH_2-MVAEDAPVRATCRVLFR-COOH) that does not contain a tyrosine residue, and this makes the mechanism and pathway by which HN is internalized interesting.

In this study we have examined the pathway of endocytosis and the ultimate fate of internalized HN protein by using immunofluorescent analysis, electron microscopy (EM) immuno-cytochemistry, and biochemical methods. We find that HN glycoprotein is concentrated and internalized in coated pits whereas the F glycoprotein remains on the cell surface.

MATERIALS AND METHODS

Cells and Virus

CV-1 cells were maintained in DMEM supplemented with 10% fetal calf serum (FCS). The W3A strain of SV5 was grown in MDBK monolayer cultures as previously described (Paterson *et al.*, 1984). SV5 infection of CV-1 cells was carried out as described previously (Ng *et al.*, 1989). CV-1 cells infected with SV5 or hPIV-3 (multiplicity of infection of ~18) were used at 15–17 h post-infection (p.i.) for all studies unless otherwise noted. The type 3 strain of human parainfluenza virus (hPIV-3) was grown in LLC-MK2 monolayer cultures as described previously (van Wyke Coelingh and Tierney, 1989). Infection of CV-1 cells with recombinant SV40 stocks expressing the cDNAs of HN, F, influenza virus hemagglutinin (HA) (A/Japan/305/57), and HA-Y543, a derivative of HA that contains a substitution of cytoplasmic cysteine residue 543 for tyrosine (Lazarovits and Roth, 1988), was done as described previously (Ktistakis *et al.*, 1990).

Indirect Immunofluorescence Microscopy

Indirect immunofluorescence microscopy was performed as described previously (Ng *et al.*, 1989), except cells were permeabilized with 0.1% saponin in phosphate-buffered saline (s-PBS) where in-

dicated. All steps were carried out at room temperature except where indicated. For confocal microscopy, CV-1 cells grown on coverslips were infected with SV5 or hPIV-3. At 13 h p.i., a Texas Red conjugate of ovalbumin (ova-TR) (Molecular Bioprobes, Eugene, OR) was added to the culture medium at a final concentration of 100 μg/ml, and cells were incubated at 37°C for 90 min. Cells were washed twice in PBS at 4°C and incubated for 30 min with either ascites fluid containing SV5 HN-specific monoclonal antibody (mAb) (HN-5a) or a pool of monoclonal antibodies specific for hPIV-3 HN (451/4 and 170/7) diluted 1:300 in 1% bovine serum albumin in PBS (BSA-PBS). Coverslips were washed in PBS at 4°C and returned to culture dishes containing ova-TR as before and incubated at 37°C for the indicated times. At each time point, cells were washed in PBS, fixed for 5 min in 0.5% formaldehyde, washed in s-PBS, and incubated for 30 min in fluorescein-conjugated goat anti-mouse IgG (Cappel, Durham, NC) diluted 1:100 in BSA-PBS containing 0.1% saponin. Cells were washed in s-PBS, then in PBS. Coverslips were mounted on slides using Mowiol containing 10% DABCO (Sigma, St. Louis, MO) and viewed using a confocal microscope (MRC 600, Bio-Rad, Richmond, CA). Images were analyzed using Adobe Photoshop. In all experiments, HN fluorescent patterns are green, and ova-TR patterns are red. Overlap between superimposed images of the two staining patterns appear yellow.

Internalization Assay

SV5-infected cells at 14–16 h p.i. were incubated in cysteine- and methionine-deficient DMEM and labeled with Tran[^{35}S]-label for 30 min. Cells were incubated for 60 min at 37°C in DMEM to permit transport of newly synthesized HN to the cell surface and then chilled to 4°C. Cell surfaces were biotinylated 3 times for 10 min each time in 0.5 ml PBS, pH 8.0, containing 1.5 mg/ml NHS-SS-biotin (Pierce, Rockford, IL) (Hunziker *et al.*, 1991) and the reaction was quenched by incubating cells in 50 mM NH_4Cl in PBS (Le Bivic *et al.*, 1989). Cells were returned to 37°C to allow internalization, and at the indicated times cells were treated three times for 30 min each with 10 mM 2-mercapto-ethanesulfonic acid (MESNa) in MESNa buffer (50 mM Tris-HCl pH 8.6, 100 mM NaCl, 1 mM EDTA, 0.2% BSA) to remove remaining surface-associated biotin and then treated with 125 mM iodoacetamide to block sulfhydryl groups (Smythe *et al.*, 1992). Cell lysates were prepared, and HN and F were immunoprecipitated as described (Ng *et al.*, 1989) with polyclonal antiserum against SDS-denatured HN or affinity-purified anti-F tail peptide antiserum. Streptavidin-agarose recovery of biotinylated HN was done as described (Le Bivic *et al.*, 1989) and polypeptides were analyzed on SDS-PAGE as described (Ng *et al.*, 1989). Gels were exposed to Fujix imaging plates and the photo-stimulated luminescence was quantified using a Fujix bio-imaging system and MacBAS software.

CV-1 cells infected with SV40 recombinant viruses expressing HN, HA, or HA-Y543 were used for experiments at 40–44 h p.i. Infected cell cultures expressing HA or HA-Y543 were labeled with Tran[^{35}S]-label for 10 min (HA and HA-Y543) or 20 min (HN), incubated in DMEM for 30–40 min (HA or HA-Y543) or 60 min (HN) to allow transport of the glycoproteins to the cell surface. Surface-expressed proteins were biotinylated and quenched as described above, and for cultures expressing HA or HA-Y543, cell surfaces were treated at 4°C with TPCK-trypsin (L-(tosylamido 2-phenyl) ethyl chloromethyl ketone-treated trypsin; Worthington Biochemical, Freehold, NJ) (100 μg/ml) to cleave residual cell surface–associated HA_0 to HA_1 and HA_2 using the protocols described by Ktistakis *et al.* (1990). For cultures expressing HN, cell surfaces were treated with MESNa as described above. Lysates were immunoprecipitated with rabbit polyclonal antiserum specific for influenza virus HA or HN. Streptavidin-agarose recovery of biotinylated proteins and quantification of radioactivity in gels was performed as described above. Uncleaved HA_0 in trypsin-treated samples was taken to represent internalized HA_0.

EM and Cytochemistry

Preparation of Gold Probes. Colloidal gold and gold-antibody conjugates were prepared essentially as described by Slot and Geuze (1985). Transferrin-gold probes of either 6- or 15-nm diameter were prepared based on a previously published protocol (Woods *et al.*, 1989). Highly iron saturated transferrin (Boehringer Mannheim, Indianapolis, IN) was used and the gold-labeled transferrin was used immediately following preparation. BSA was coupled to 6 nm colloidal gold according to the method of Ghitescu *et al.* (1986).

Immunocytochemical Staining of Cell Monolayers. To examine the internalization of HN monolayers of SV5-infected CV-1, cells at 17 h p.i. were washed with PBS at 4°C and incubated with ascites fluid containing either the HN-specific mAb HN5a or the F-specific mAb F1a (Randall *et al.*, 1987) (diluted 1:300 in DMEM containing 10 mM *N*-2-hydroxyethylpiperazine-*N*′-2-ethanesulfonic acid [HEPES], pH 7.3) for 1 h at 4°C. Cultures were then washed with several changes of DMEM containing 10 mM HEPES, pH 7.3, at 4°C over 15 min. Antibody binding was visualized by staining monolayers for 1 h at 4°C with goat anti-mouse IgG (Jackson Immunoresearch, West Grove, PA) coupled to 10 nm colloidal gold unless otherwise noted. Gold-labeled secondary antibody was used, diluted to an OD_{520} = 3.0; we found the relatively high concentration was necessary to stain HN on the cell surface in addition to staining the more antibody-accessible budding virus. Cells were washed as above and then placed in DMEM supplemented with 2% FCS pre-warmed to 37°C (0 min). At the times indicated, cultures were washed several times with PBS, and fixed for 2 h in 2% glutaraldehyde, and post-fixed for 1 h in 1% osmium tetroxide, both in 0.1 M phosphate buffer, pH 7.4. Cells were dehydrated at room temperature through a graded ethanol series. The final step of dehydration in propylene oxide also released the monolayer from the plastic culture dish. Cells were infiltrated and embedded in epoxy resin, thin sections were collected on parlodion-coated 200 mesh copper grids, contrasted with uranyl acetate and lead citrate, and examined in a Jeol JEM-100CX II EM operating at 80 kV. For controls, mock-infected cells were stained as detailed above and SV5-infected cells were stained with the gold-coupled secondary antibody alone.

To co-localize HN and transferrin, SV5-infected CV-1 cells were rinsed three times with DMEM containing 10 mM HEPES, pH 7.4, and then incubated at 37°C for 30 min in DMEM minus serum. The monolayers were washed once in DMEM plus 10 mM HEPES, pH 7.4, at 4°C, and then incubated for 1 h at 4°C with mAb HN5a diluted 1:300 in the same medium. The cells were rinsed three times over 15 min in DMEM containing 10 mM HEPES then incubated at 4°C for 1 h simultaneously with goat anti-mouse IgG conjugated to 15 nm gold particles and transferrin coupled to 6 nm gold. After washing as above, the dishes were flooded with pre-warmed DMEM plus 10 mM HEPES, containing transferrin-gold probe at a 1:10 dilution and incubated for varying times at 37°C. Finally cells were washed and fixed as described above. As a control, cells were initially incubated for 30 min at 37°C with unconjugated transferrin at a 7.5-fold excess over the concentration of gold-conjugated transferrin and then processed as described above.

To examine the localization of BSA-gold complexes simultaneously with internalized HN, subconfluent CV-1 cells were washed with PBS, infected with SV5 as described above, and then incubated at 37°C overnight in DMEM supplemented with 2% FCS in the presence of BSA coupled to 6 nm gold (used at a final dilution of 1:7.5). Subsequently monolayers were stained for HN, incubated for 4 h at 37°C, and then processed for EM as described above.

Cytosolic Acidification of SV5-infected CV-1 Cells. The acidification of the cytosol of SV5-infected CV-1 cells was based upon the protocol described by Sandvig *et al.* (1987). After staining cells at 4°C with mAb HN5a and 10 nm gold-coupled secondary antibody as described above, cultures at 4°C were incubated for 30 min with 30 mM NH_4Cl in DMEM + 10 mM HEPES, pH 7.4, followed by a 5-min incubation at 4°C in Na^+-free buffer (140 mM KCl, 2 mM $CaCl_2$, 1 mM $MgCl_2$, 1 mM amiloride, 10 mM HEPES, pH 7.4)

(Fuhrer *et al.*, 1991). Cells were placed in pre-warmed 37°C Na^+-free buffer in a CO_2 incubator for 90 min, and then fixed and processed for EM as described above. For comparison, duplicate cultures were stained and processed in parallel without NH_4Cl pulse or amiloride treatment and incubated for 90 min in DMEM + 10 mM HEPES, pH 7.4.

Immunocytochemical Staining of Permeabilized Cells. Cultures of SV5-infected CV-1 cells were rinsed twice with DMEM containing 10 mM HEPES, pH 7.4, at 37°C and then incubated in the same medium for 30 min at 37°C. Cells were washed in DMEM containing 10 mM HEPES, pH 7.4, at 4°C and incubated for 1 h at 4°C with transferrin coupled to 15 nm gold particles diluted 1:10 in DMEM plus 10 mM HEPES. Cells were washed and then incubated in pre-warmed DMEM containing 10 mM HEPES and 100 μg/ml cycloheximide, and incubated for 90 min at 37°C. Following washing, cells were fixed for 30 min with freshly prepared periodate-lysine-paraformaldehyde fixative (McLean and Nakane, 1974), washed in PBS, and then permeabilized by treatment for 15 min with 0.1% s-PBS. Monolayers were stained for 1 h with gentle rocking with either mAb HN5a or mAb F1a, diluted 1:300 in s-PBS. Following washes with multiple changes of s-PBS over 30 min, antibody binding was visualized by a 1-h incubation in goat anti-mouse IgG coupled to 6 nm gold particles diluted as previously stated in s-PBS. Cells were washed with s-PBS for 30 min and then fixed with glutaraldehyde, post-fixed with osmium tetroxide, dehydrated, and embedded as above.

Quantification of Gold Staining

Quantification of gold labeling was carried out based upon the principles described by Weibel (1979). Sections from different depths of a tissue block were used and where possible multiple blocks were used. Cells to be photographed were randomly selected. As CV-1 cells grown in monolayer are thin and flat, micrographs included the entire thickness of the cell where possible. Prints were enlarged to a final magnification of 20,000 and were randomly overlaid with a grid corresponding to a 1-μm lattice. The gold particles decorating the cell surface but not on progeny viruses were counted using a 10× magnifier, and intersections of the cell membrane with the overlaid grid were noted. Only the apical surface of the cell was measured and counted because the basal surface was adherent to the culture dish during staining and therefore exhibited a greatly reduced level of labeling. Coated pits were noted, and any gold contained within them was counted. Internalized gold observed within intracellular structures was also counted. The length of cell membranes examined in each case ranged from 150 to 350 μm, with the total number of gold particles counted ranging from 2,264 to 8,076, excluding the negative control (19 gold particles total).

Reagents

Chemicals were purchased from Sigma (St. Louis, MO) unless otherwise stated; EM supplies were from Electron Microscopy Sciences (Fort Washington, PA).

RESULTS

SV5 HN but not HPIV-3 HN Is Internalized from the Surfaces of CV-1 Cells and Localized to Endocytic Compartments

The degree to which the HN glycoprotein in SV5-infected cells co-localized with a marker for fluid-phase internalization (ova-TR) was assessed by using indirect immunofluorescent confocal microscopy (Figure 1). It has been shown previously that internalization of HN is independent of bound antibody (Ng *et al.*, 1989), thus surface-bound HN antibody can be used to follow internalization of HN molecules. Ova-TR is nonspecifically internalized by cells and enters the endocytic pathway (Lippincott-Schwartz and Fambrough, 1987). SV5- and hPIV-3-infected CV-1 cells at 13 h p.i. were incubated with ova-TR for 90 min, and then chilled to 4°C and incubated with mAbs specific for SV5 or hPIV-3 HN. Excess antibody was removed by washing, and coverslips were incubated at 37°C in medium containing ova-TR. At each time point, cells were fixed and permeabilized. HN glycoprotein was detected using a goat anti-mouse fluorescein conjugate. At all time points, ova-TR stained clusters of large vesicles in the vicinity of the nucleus (Figure 1). SV5-infected cells kept at 4°C after incubation with the primary antibody (0 min) showed staining of HN at the plasma membrane; finger-like projections from the membrane of cells are presumed to be budding filamentous SV5 virions. After 30 min at 37°C, the SV5-infected cells showed HN staining in small, vesicular structures at the periphery of the cell that were largely devoid of ova-TR. However, after 90 min at 37°C the SV5 HN staining pattern significantly overlapped that of ova-TR. In contrast, the hPIV-3 HN staining pattern showed a high degree of patching at the cell surface at all time points with no overlap between the HN pattern and the ova-TR pattern, indicating that hPIV-3 HN is not internalized from the infected cell surface. This difference in internalization phenotype between HN proteins of highly related viruses suggests that the internalization of SV5 HN may be directed by a determinant within the SV5 HN molecule.

Intracellular Accumulation and Turnover of Surface-biotinylated SV5 HN Protein

Pulse-chase experiments with metabolically labeled SV5-infected CV-1 cells showed that the amount of HN immunoprecipitated decreased with time of chase at 37°C (Ng *et al.*, 1989). To examine further the apparent loss of HN from the surface of infected cells, cultures were metabolically pulse-labeled and chased to allow transport of newly synthesized protein to the cell surface. Cells were chilled, biotinylated using the disulfide cleavable reagent NHS-SS-biotin, and re-

Figure 1 (facing page). SV5 HN is internalized and co-localizes with intracellular vesicles containing internalized ovalbumin. SV5- and hPIV-3-infected CV-1 cells grown on coverslips at 13 h p.i. were incubated for 90 min at 37°C in the presence of 100 μg/ml ovalbumin conjugated to Texas Red (ova-TR). Cells were washed in PBS at 4°C to inhibit endocytosis and the cell surface was stained with mAbs specific for SV5 or hPIV-3 HN. Coverslips were washed and returned to the culture media containing ova-TR at 37°C. After 0, 30, and 90 min at 37°C, cells were washed, fixed with paraformaldehyde, permeabilized with 0.1% saponin in PBS, and incubated with

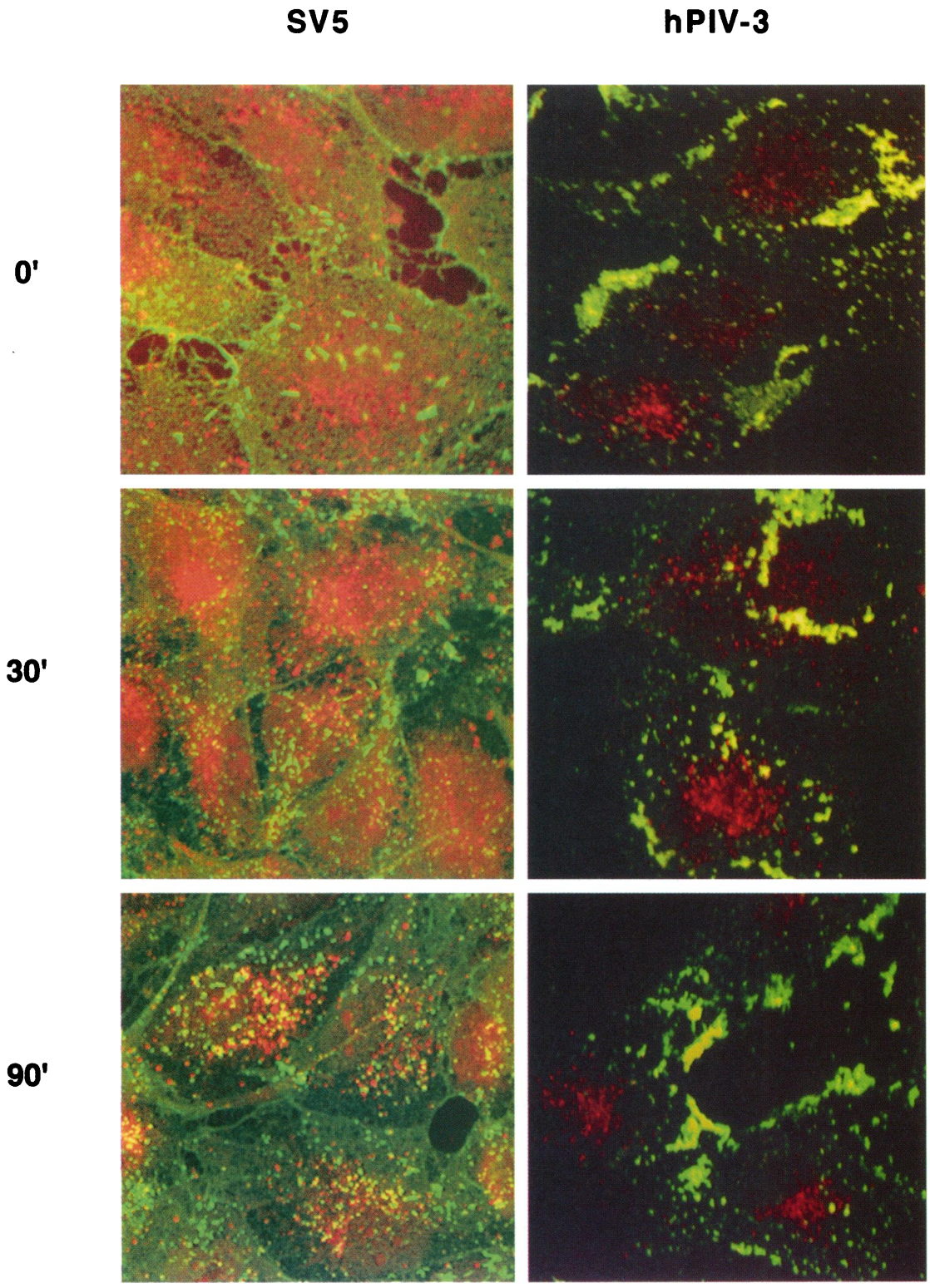

(Figure 1 cont.) goat anti-mouse IgG fluorescein conjugate in 0.1% saponin and 1% BSA in PBS. Coverslips were washed, mounted, and examined with a confocal microscope. The images were computer processed and color was added. HN staining appears green, ova-TR fluorescence appears red, and areas of co-localization appear yellow. For hPIV-3 panels, the fluorescein staining was so intense that there was some bleed-through in the rhodamine channel at all time points (due to the design of the MRC 600 confocal microscope [Bio-Rad]), and thus the fluorescein staining appears yellow.

turned to 37°C for varying times. The fates of surface HN and F glycoproteins were examined by immunoprecipitation using HN- or F-specific antisera and streptavidin-agarose recovery. Intracellular accumulation of SV5 HN reached a steady state level of ~25% after 60 min of chase (Figure 2A). Loss of total HN mirrored the internal accumulation such that 75% of total HN was recovered at 60 min of chase. However, after 90 min of chase, loss of HN continued but internal accumulation remained at 25%, suggesting that internalized HN was degraded (Figure 2A). SV5 F glycoprotein could not be recovered internally at any time point, and no significant loss in total radioactivity was observed (Figure 2A). Time courses of degradation of SV40-expressed F and HN are shown in Figure 2B. The amount of HN immunoprecipitated decreased steadily from 1–7 h of chase, and two degradation products, p34 and p27, appeared as transient species. In contrast, the amount of F protein immunoprecipitated remained constant. During the time course, the precursor F_0 was cleaved to the disulfide-linked oligomer F_1/F_2; the disappearance of F_0 and the appearance of the membrane-anchored F_1 subunit are shown (Figure 2B, right panel).

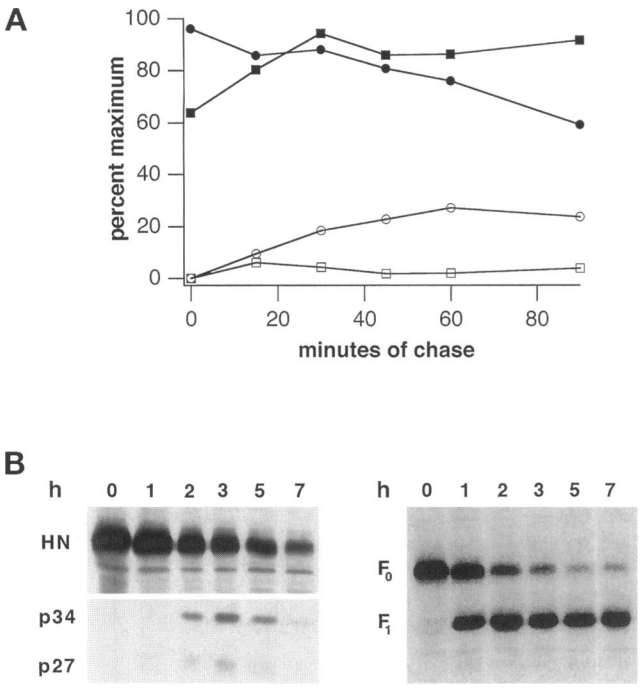

Figure 2. Distribution of surface-biotinylated HN and F glycoproteins. Cell cultures were labeled with Tran[^{35}S]-label for 30 min and chased for 60 min to allow newly synthesized HN and F to reach the cell surface. Cultures were biotinylated at 4°C using cleavable disulfide reagent NHS-SS-biotin, and cultures were returned to 37°C to allow internalization. At each time point cultures were treated with the membrane impermeant-reducing agent MESNa, and biotinylated proteins were isolated by immunoprecipitation and streptavidin-agarose recovery. (A) Total SV5 HN (closed circles) and SV5 F (closed squares) are plotted as a percentage of maximum radioactivity recovered over the time course. Internal SV5 HN (open circles) and SV5 F (open squares) from MESNa-treated cultures are plotted as a percentage of biotinylated material present at 0 min. (B) HN- or F-expressing cultures were labeled for 20 min with Tran[^{35}S]-label and chased for the indicated periods of time, and lysates were immunoprecipitated. P34 and p27 are degradation products of HN. The precursor F_0 is cleaved to the disulfide-linked oligomer F_1/F_2, only the membrane-anchored F_1 subunit is shown.

The efficiency of internalization of HN (Figure 3C) was assessed by comparison with the efficiency of internalization of influenza virus HA-Y543 (Figure 3B) and wild-type (wt) HA (Figure 3A). HA-Y543 contains a tyrosine for cysteine substitution in its cytoplasmic tail and has been extensively characterized and shown to be endocytosed at rates similar to those of cell surface receptors (Lazarovits and Roth, 1988). wt HA is expressed stably at the cell surface and provides a marker for basal membrane turnover (Ktistakis *et al.*, 1990; Thomas *et al.*, 1993). HN, wt HA, and HA-Y543 were expressed from cDNAs using SV40-recombinant viruses and infected cell surfaces were biotinylated with NHS-SS-biotin at 4°C as described in MATERIALS AND METHODS; cultures were warmed to 37°C for varying periods to allow for internalization of biotinylated protein, and returned to 4°C. Cells expressing HN were treated with MESNa to remove remaining cell surface–associated biotin and cells expressing HA and HA-Y543 were treated with TPCK-treated trypsin to cleave residual cell surface–associated HA_0 to HA_1 and HA_2 (Ktistakis *et al.*, 1990). The total

Figure 3 (facing page). Comparison of the internalization of HN with wt HA and mutant HA-Y543. CV-1 cells infected with SV40 recombinant viruses expressing wt HA, HA-Y543, and HN were labeled with Tran[^{35}S]-label for 10 min (HA and HA-Y543) or 20 min (HN) and cultures were then incubated in DMEM to allow for newly synthesized proteins to be transported to the cell surface (HA and HA-Y543, 30–40 min; HN, 60 min). Cultures were placed at 4°C, proteins were biotinylated with NHS-SS-biotin, and then cultures were returned to 37°C for the times indicated to permit internalization. At each time point, cultures were treated with TPCK-trypsin (wt HA and HA-Y543) or MESNa (HN), and biotinylated proteins were isolated by immunoprecipitation using HA- or HN-specific sera and biotinylated molecules were recovered using streptavidin-agarose as described in MATERIALS AND METHODS. (A, left panel) Total labeled wt HA isolated at each time point (squares), wt HA protected from trypsin cleavage (circles), and total wt HA internalized and degraded (dashed line with triangles). (A, right panel) Image of radioactivity on gel using Fujix Bio-Imaging system to show time course of wt HA internalization. (B; left panel) Total labeled HA-Y543 at each time point (squares), HA-Y543 internalized and resistant to trypsin cleavage (circles) and the total HA-Y543 internalized and degraded (dashed line with triangles). (B, right panel) Image of radioactivity on gel using Fujix Bio-Imaging system to show time course of HA-Y543 internalization. (C, left panel) Total labeled HN (squares), HN internalized and protected from the reducing agent MESNa (circles) and the total HN internalized and degraded (dashed line with triangles). (C, right panel) Image of radioactivity on gel using Fuji Bio-Imaging system to show time course of HN internalization. Note the presence of transient degradation fragments (p34) at later time points.

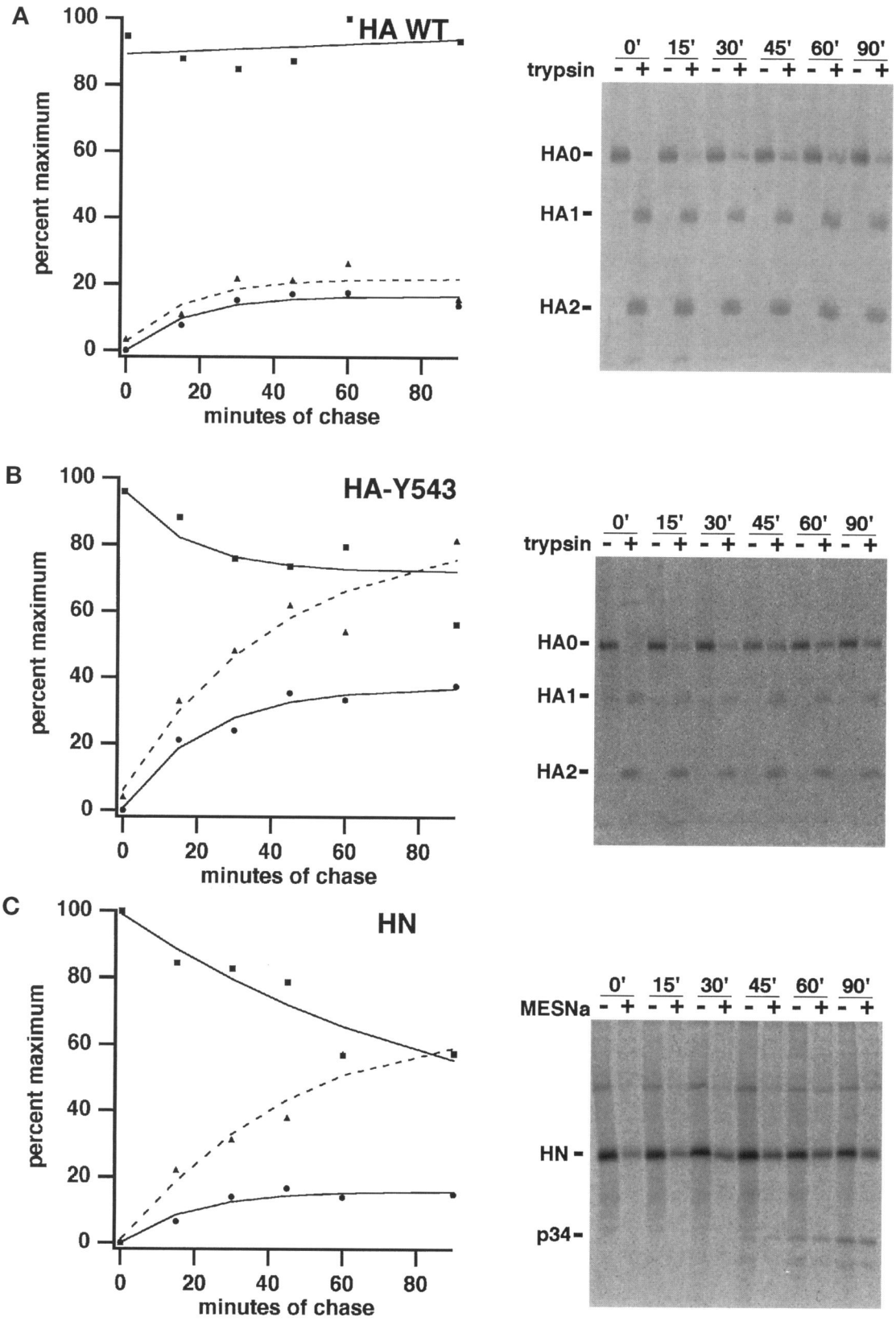

Figure 3 (cont).

amount of labeled wt HA (Figure 3A, squares) remained relatively stable, while both HA-Y543 (Figure 3B, squares) and HN (Figure 3C, squares) showed substantial loss of labeled protein due to internalization and degradation. The HA or HA-Y543 molecules that were protected from trypsin cleavage, and for HN the biotinylated molecules recovered after MESNa treatment, represented molecules internalized into cells (Figure 3, circles). To compare the relative internalization efficiencies of HA, HA-Y543, and HN the amount of label lost due to degradation was added to the amount internalized at each time point (Figure 3, triangles). The total amount of HN internalized over the course of the experiment was slightly lower than that for HA-Y543, with 50% HN internalized in 50 min and ~50% HA-Y543 internalized in 30 min. However, these values are significantly higher than wt HA, which showed less than 20% of the total protein internalized over the course of the experiment (90 min).

HN Is Internalized Via Clathrin-coated Pits

The cellular pathway of internalization of HN glycoprotein was examined by using immuno-electron microscopy. SV5-infected CV-1 cells were chilled to 4°C to inhibit endocytosis and labeled with HN-specific mAb followed by secondary IgG conjugated to 10 nm gold particles. Following incubation for varying times at 37°C, cell cultures were fixed and prepared for examination in the electron microscope. CV-1 cells fixed at 0 min showed extensive gold labeling of the cell surface but no gold particles were observed within the cell (Figure 4A). After 15 min at 37°C, there was extensive labeling of the cell surface and some HN was observed in early endosomes (Figure 4B, arrow): endosomes are identified by their uncoated vacuole-like appearance and mostly reside in the peripheral cytoplasm (Griffiths *et al.*, 1989). Note the presence of gold label in a coated pit (Figure 4B, CP). Following 30 min (Figure 4C) at 37°C, labeled SV5-infected CV-1 cells showed progressively less HN cell surface staining, while the amount of label that accumulated in endosomal compartments increased (Figure 4C, arrow). After 2 h at 37°C, labeled HN present on the cell surface had been further reduced, and heavily labeled endosomes were frequently observed (Figure 4D). A labeled progeny virus particle is visible in this micrograph (Figure 4D, V). With longer periods of incubation at 37°C, labeled endosomes were marked by increasing amounts of internal material, a generally denser appearance (underscored by the aggregated appearance of the gold label in the vesicles), and a juxanuclear location within the cell (Neutra *et al.*, 1985; van Deurs *et al.*, 1993b). These structures frequently contained multiple small vesicles believed to be derived from the delimiting membrane and are termed multiple vesicular bodies (Hirsch *et al.*, 1968). Stained SV5 virions were observed in clathrin-coated pits, and intact viral particles (identifiable by their distinctive morphology) were occasionally found in endosomes. HN was found concentrated in cellular structures possessing the dense, filled, and compacted morphology of late endosomes/lysosomes after 4 h at 37°C (Figure 4E, arrows). In these dense structures the gold particles were found to be quite aggregated: note also the heavily labeled multivesicular body that contains a myelin figure (Figure 4E, arrowhead), a common morphological marker of late endosomes (van Deurs *et al.*, 1993a). Much less cell surface labeling of HN was observed at this stage; however, when it was encountered it tended to be localized to discrete areas.

Previous immunofluorescent staining data indicated that the other SV5-expressed glycoprotein F was not internalized (Ng *et al.*, 1989). We therefore used examination of F protein by immuno-gold labeling as a control for the HN-labeling pattern. SV5-infected CV-1 cells were stained with F-specific mAb F1a followed by gold-conjugated secondary IgG and the cells were returned to 37°C as described for anti-HN stained cells. After extended chase periods at 37°C, gold-labeled F remained predominantly at the cell surface (compare the extent of cell surface labeling of F [Figure 4F] after 120 min at 37°C to that of HN [Figure 4D] for the same time period). Gold-labeled F in endosomes was found infrequently.

SV5-infected CV-1 cells stained with mAb HN5a showed a large number of clathrin-coated pits and coated vesicles labeled with gold particles. Examination of cells showed coated pits in various stages of invagination and displayed the characteristic electron dense coat (Figure 5, A–E). The panels shown represent cells incubated for 15 min at 37°C; however, all time points examined provided similar examples. Careful examination of membrane invaginations having characteristics consistent with caveolae (i.e., smaller than coated pits, no visible electron dense coat, flask shaped, and frequently found in clusters) (Ghitescu *et al.*, 1986; Fujimoto, 1993) revealed no labeling (Figure 5F). Highly convoluted regions of plasma membrane occasionally were observed, usually associated with regions of virus budding. Internalization of gold particles by apparent membrane ruffling or infolding was observed a total of two to three times in all specimens examined, and was always associated with highly localized areas of membrane convolution. This was not seen with enough frequency to account for the observed level of HN internalization. Mock-infected CV-1 cells when stained with mAb HN5a, followed by gold-coupled secondary IgG and processing for EM after either 0 or 90 min at 37°C, showed almost no labeling of the cell surface (see Table 1) and a total absence of internal gold staining.

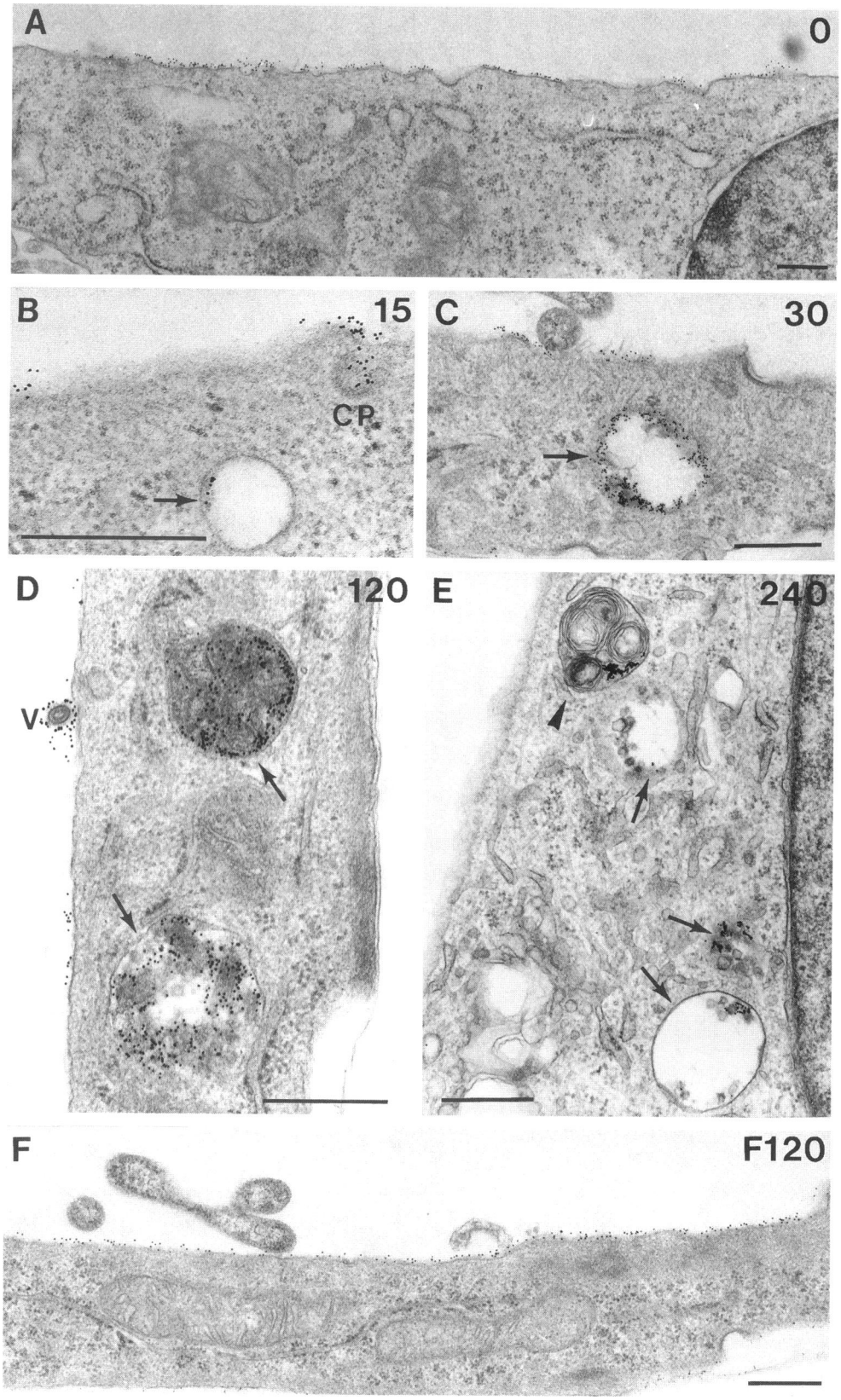

Figure 4. Morphological examination of HN internalized from the cell surface. SV5-infected CV-1 cells were washed with PBS at 4°C and cell surfaces incubated with mAbs specific for either HN (HN5a) or F (F1a) for 1 h, washed with PBS, followed by a 1 h incubation in goat anti-mouse Igs coupled to 10 nm gold particles. After washing with PBS, cells were incubated at 37°C for varying times. Cells were then fixed with glutaraldehyde followed by post-fixation in osmium tetroxide. Following dehydration in a graded ethanol series, cells were embedded in Epon, and thin sectioned. Sections were contrasted with uranyl acetate and lead citrate. A profile of a cell stained for HN and fixed without incubation at 37°C, effectively a 0 time point, is shown in panel A. Cells incubated for 15, 30, 120, and 240 min at 37°C before fixation are shown in panels B, C, D, and E, respectively. A cell stained with mAb F1a that was incubated at 37°C for 120 min before processing for EM is shown in panel F. Arrows denote endosomal vesicles containing HN. V, stained progeny virus; CP, coated pit; arrowhead, labeled multivesicular body containing myelin figure. Bar, 0.5 μm.

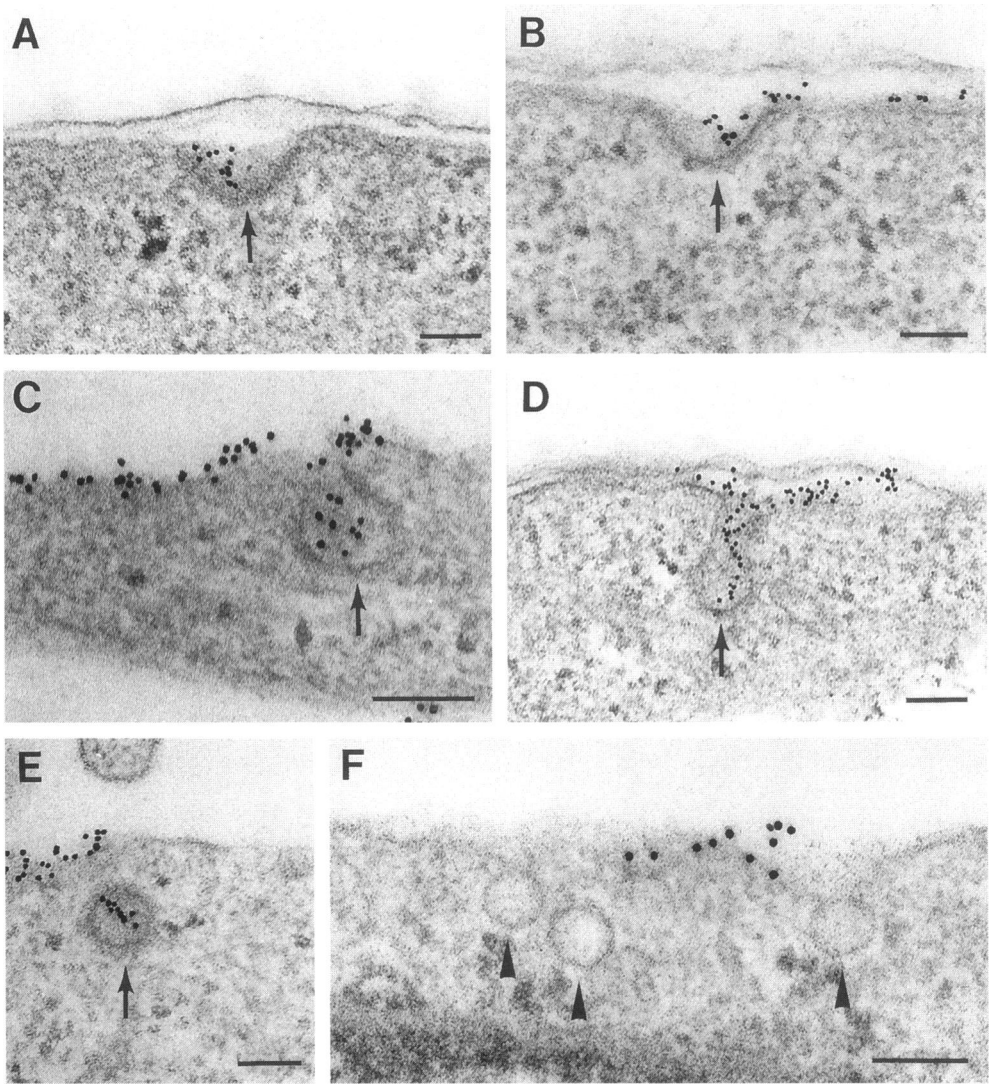

Figure 5. HN on the plasma membrane localizes to coated pits. SV5-infected CV-1 cells were washed with pre-chilled PBS and placed at 4°C to inhibit endocytosis. Cells were stained with mAb HN5a for 1 h at 4°C, and washed several times with PBS, followed by a 1 h incubation with a secondary antibody coupled to 10 nm colloidal gold. Following extensive washing with PBS at 4°C, cells were placed in pre-warmed 37°C DME + 10 mM HEPES, pH 7.4, for 15 min and then processed for EM. Clathrin-coated pits (arrow) in varying stages of invagination that contain gold-labeled HN glycoprotein are shown in panels A–E. Invaginations (arrowheads) consistent with the physical properties of caveolae on the surface of HN-stained SV5-infected CV-1 cells incubated at 37°C for 15 min are shown in panel F. Bar, 0.1 μm.

Quantification of Gold Labeling

The distribution of gold-labeled HN was quantified by randomly photographing sections of SV5-infected CV-1 cells that had been reacted with viral protein-specific antibodies and prepared for EM as described above. Prints were made with a final magnification of 20,000 and the membrane length of cell profiles was estimated by counting membrane intersections with a

Table 1. Quantification of gold labeling

	HN					F		Mock
min 37°C	0	15	30	60	90	0	90	90
Gold/100 μm cell membrane	2153	1591	1328	1004	854	2241	2006	10.8
Coated pits/100 μm cell membrane	8.5	6.1	11.9	9.5	12.2	14	8.7	7.9
Gold in coated pits/100 μm cell membrane	18	74	80.4	49.4	44.1	1.2	3.6	0
Percent coated pits labeled	61	88	48.7	42	38	8.6	19	0
Gold in endosomes/100 μm cell membrane	0	22	415	534	1232	0.6	271	0
Percent gold on cell surface in coated pits	0.83	4.7	6.1	4.9	5.2	0.05	0.18	0
Total gold counted	3330	2264	6047	3986	3643	3766	8076	19

grid (Weibel, 1979). Only gold particles on the plasma membrane were counted. HN protein contained within progeny virions were not counted because this population of HN would be expected to have restricted movement in the plane of the membrane. Areas of virus budding exhibited bristle-like patches of viral glycoproteins F and HN, and HN protein contained within these areas would not be expected to be free to move into coated pits; however, gold staining of these patches was counted because it was difficult to consistently identify these areas. SV5-infected cells stained with mAb HN5a showed an increase in gold in the endocytic compartments with increasing incubation times at 37°C (Table 1). As the amount of HN decreased on the surface there was an accompanying increase in label observed in endosomal compartments. The amount of label observed in clathrin-coated pits following incubation at 37°C ranged from 4.7 to 6.1% of total gold counted, but was constant at ~5% of the gold label present on the cell surface. A higher percentage of label in coated pits has been reported for some cell surface receptors, however, the amount of total label in those studies did not approach that seen here when staining the virally expressed HN protein. The percentage of coated pits that were labeled varied from a high of 88% after 15 min to 38% after 90 min. The number of labeled coated pits increased from 0 to 15 min most likely due to the inability of antibodies to penetrate the more highly invaginated coated pits and bind to already sequestered HN molecules at 0 min. The inaccessibility of some coated pits to penetration by antibodies has been described in the case of transferrin receptors (Schmid and Smythe, 1991). Quantification of internalized HN in cells incubated beyond 90 min at 37°C was hampered by the aggregated nature of the gold label in some of the late endosomes. While a small amount of gold was observed within cells stained with mAb F1a following 90 min at 37°C (11.9% of total), it was 80% less than the amount of gold internalized in HN-stained cells for the same time period (59% of total). The small amount of F within cells likely represents F protein internalized through membrane infolding and turnover. Mock-infected cells stained with HN-specific antibodies showed almost no surface staining (19 gold particles/176 μm of membrane) and no internalized gold particles.

Co-localization of Internalized HN with Markers for Early and Late Endosomal Compartments

As discussed above, gold-labeled HN was observed entering the endosomal system via clathrin-coated pits. To determine more rigorously the identity of the structures in which internalized HN was observed, cells were double-stained for HN and for established markers for early endosomal and late endosomal/lysosomal compartments.

SV5-infected CV-1 cells were stained with HN-specific mAbs and incubated in the presence of gold-conjugated transferrin, a molecule known to be internalized via coated pits into early endosomes and sorted for recycling back to the cell surface (Hopkins and Trowbridge, 1983; Neutra *et al.*, 1985). Examination of thin sections showed a co-localization of HN-gold (15 nm) with transferrin-gold (6 nm) (Figure 6A, arrows). Note in Figure 6A (arrowhead) the coated pit that exhibited the distinctive striated electron-dense coat under the membrane surface and was labeled with transferrin-gold (6 nm) while HN-gold (15 nm) was seen on the edge of the invagination. Internalization of transferrin-gold was reduced 91% by prior incubation of the cells with a 7.5-fold excess of unconjugated transferrin.

It is well established that cells pinocytose BSA nonspecifically when it is added extracellularly and the cells rapidly shuttle the BSA into the endocytic pathway (Ghitescu *et al.*, 1986; Lippincott-Schwartz and Fambrough, 1987). The late endosomal/lysosomal structures of SV5-infected CV-1 cells were loaded with gold-labeled BSA by overnight incubation at 37°C as described in MATERIALS AND METHODS. The cells were then stained for HN and processed as above. It was observed that when CV-1 cells had been allowed to internalize HN for 4 h at 37°C, HN-gold (15 nm) and BSA-gold (6 nm) were both visible together (Figure 6B, arrows), often as aggregates, in structures possessing the morphology of late endosomes.

Acidification of the Cytosol Inhibits the Endocytosis of HN

It has been shown previously that endocytosis of transferrin or epidermal growth factor via clathrin-coated pits is strongly reduced by the acidification of the cytoplasm (Sandvig *et al.*, 1987). To further establish that the endocytosis of HN is clathrin-dependent, cytosol acidification was performed. SV5-infected CV-1 cells were treated with 30 mM NH_4Cl for 30 min and then incubated in Na^+-free medium in the presence of 1 mM amiloride, thus blocking the Na^+/H^+ exchanger and maintaining a reduced cellular pH. Cells were incubated at 37°C for 90 min to allow for HN internalization. Immunofluorescent localization of HN in saponin-permeabilized cells allowed staining simultaneously of both surface and internalized HN. Control cells showed internalized HN in a juxtanuclear pattern suggestive of late endosomes (Figure 7A). Following acidification, the immunofluorescence staining pattern was found to be diffuse (Figure 7B), and thought to represent mostly surface staining. Examination of control cells in the EM commonly showed a number of heavily labeled endosomes (Fig-

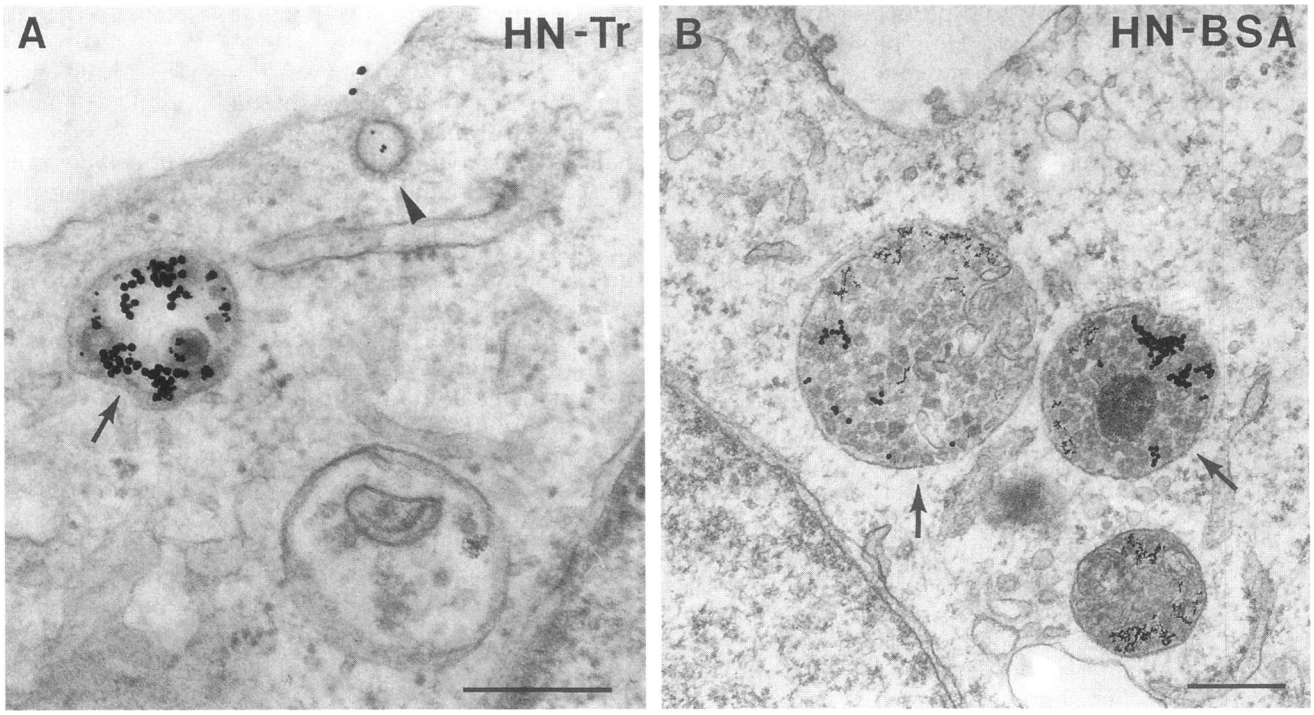

Figure 6. HN co-localizes with transferrin and BSA, markers for early endosomes and lysosomes, respectively. (A) Co-localization of HN with transferrin. SV5-infected CV-1 cells were incubated in serum-free DME for 30 min at 37°C and then chilled to 4°C to inhibit endocytosis, washed with PBS, reacted with HN-specific antibodies, washed with PBS, and stained with secondary Igs coupled to 15 nm gold particles as described in the legend to Figure 4. Following washing, cells were incubated at 37°C in DME + 10 mM HEPES, pH 7.4, containing transferrin coupled to 6 nm gold for 90 min to continuously label the endocytic pathway and the cells processed for EM. Endosomes containing HN and transferrin are shown by an arrow, and a coated pit containing transferrin with HN at the opening of the invagination is marked with an arrowhead. (B) Lysosomes were loaded with BSA by incubating SV5-infected CV-1 cells overnight at 37°C in the presence of BSA coupled to 6 nm colloidal gold. The cells loaded with BSA-gold were chilled to 4°C, stained with mAb HN5a followed by secondary coupled to 15 nm gold as described above. Cells were incubated at 37°C for 4 h and then processed for EM. Late endosomes/lysosomes containing both BSA and HN are denoted by arrows. Bar, 0.25 μm.

ure 7C, arrow) and some cell surface staining similar to what had been observed previously (see Figure 4). In contrast, cells that were treated with NH_4Cl showed the presence of HN predominantly on the cell surface (Figure 7D). Labeled endosomes were less frequently encountered and when observed they had fewer gold particles per endosome than in control cells. Quantification of the gold-labeling indicated that in acidified cells there were 701 gold particles per 100 μm of membrane length with 55 gold particles observed within endosomes for the same length of membrane (1365 total gold particles counted). Untreated cells, reacted in parallel, showed 571 and 752 gold particles on the surface or in endosomes, respectively, for 100 μm of plasma membrane (3081 gold particles total). Consistent with the idea that acidification blocks the pinching-off of coated pits to form vesicles, there was no reduction in the number of coated pits observed in treated cells; however, there was ~85% reduction in the percentage of the total label internalized (56.8% reduced to 7.8%) after 90 min at 37°C.

Direct Localization of Internalized HN

As discussed above HN internalization is not dependent upon antibody binding (Ng *et al.*, 1989). However, here it was necessary to establish that the localization of gold particles to successive compartments of the endocytic pathway represented the presence of HN in these structures and it was necessary to rule out the possibility of dissociation of primary or secondary antibodies from their respective targets upon internalization. SV5-infected CV-1 cells at 17 h p.i. were treated with cycloheximide to inhibit protein synthesis, and stained with transferrin coupled to 15 nm gold. Cells were then mildly fixed with periodate-lysine-paraformaldehyde, permeabilized with saponin, incubated with mAb HN5a or mAb F1a proteins, and finally treated with mouse-specific secondary IgG coupled to 6 nm gold. Cells were then fixed with glutaraldehyde and osmium tetroxide and processed for EM. As shown in Figure 8A (arrows), HN was localized to endosomes, which confirms that internalization is not antibody mediated and demonstrates

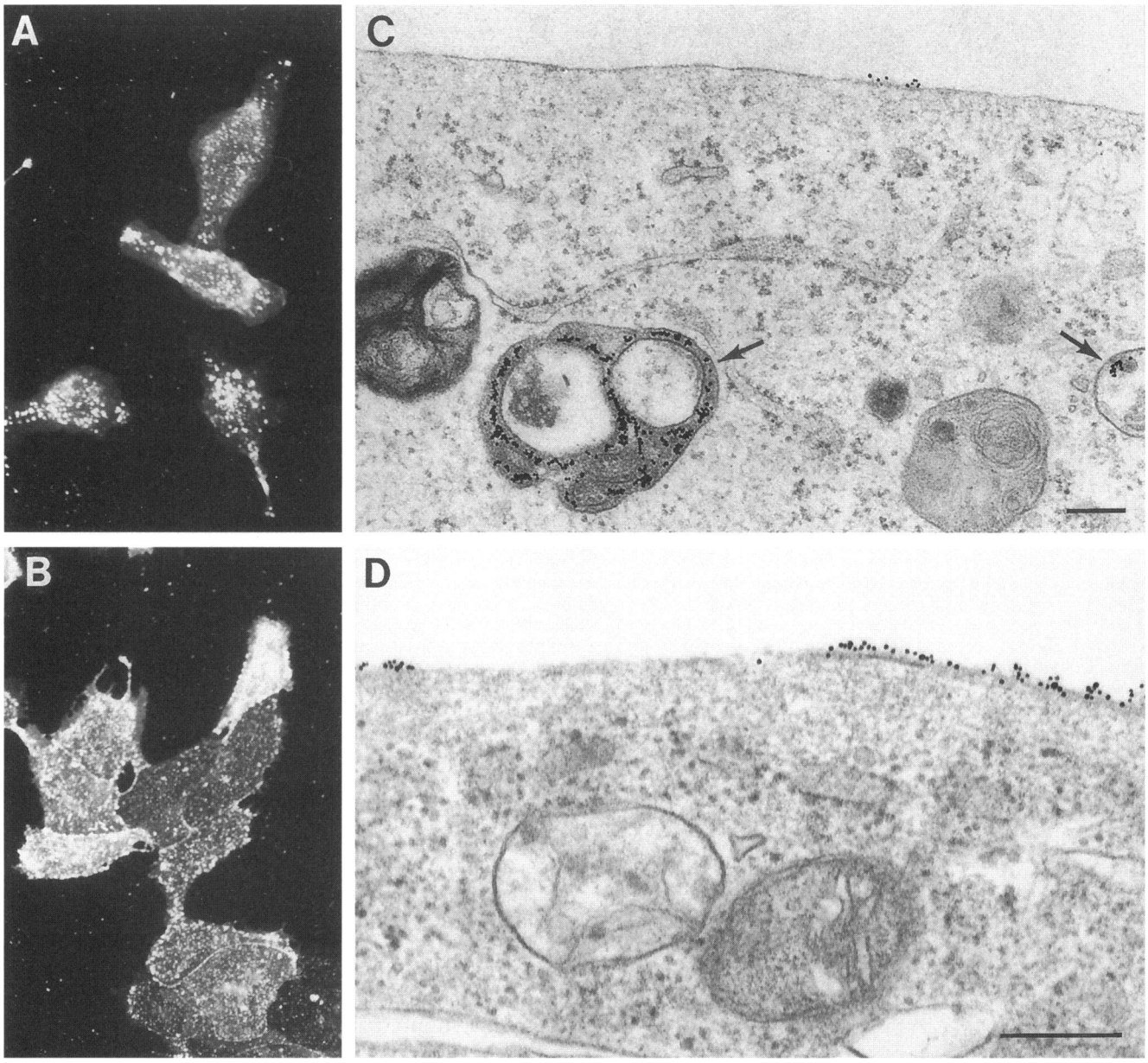

Figure 7. Cellular uptake of HN is inhibited by acidification of the cytosol. (A and B) For examination by immunofluorescence, SV5-infected CV-1 cells were washed in DME + 10 mM HEPES, pH 7.4, pre-chilled to 4°C, incubated for 1 h with mAb HN5a, and washed with DME + 10 mM HEPES, pH 7.4. Cells used in immunofluorescent experiments were either left as a control in DME, or treated for 30 min at 4°C with 30 mM NH_4Cl in DME + 10 mM HEPES, pH 7.4. Following the NH_4Cl pulse, treated cells were incubated in Na^+-free buffer containing 1 mM amiloride as described in MATERIALS AND METHODS. Both control and acidified cells were incubated at 37°C for 90 min, after which cells were fixed with formaldehyde, permeabilized with 0.1% saponin in PBS, and reacted with fluorescein-conjugated goat anti-mouse IgG. Saponin permeabilization allows the simultaneous demonstration of both surface and intracellular staining. (C and D) Cells to be processed for electron microscopy were stained for HN as described above followed by a 1-h incubation at 4°C in goat anti-mouse secondary antibody coupled to 10 nm gold particles. After washing, cells were either treated as control (C) or acidified (D) as described above. Following a 90-min incubation at 37°C cells were processed for EM. Labeled endosomes are denoted by arrows. Sections were contrasted with uranyl acetate and lead citrate. Bar, 0.25 μm.

that gold particles observed within cellular compartments represent the presence of HN. After 90 min at 37°C, HN was found in an array of endosomal structures including multivesicular bodies. Due to the incubation conditions employed and possibly the size of the gold particles, the labeling of transferrin receptors was less than observed in Figure 6A, although several 15 nm gold particles can be observed (Figure 8A,

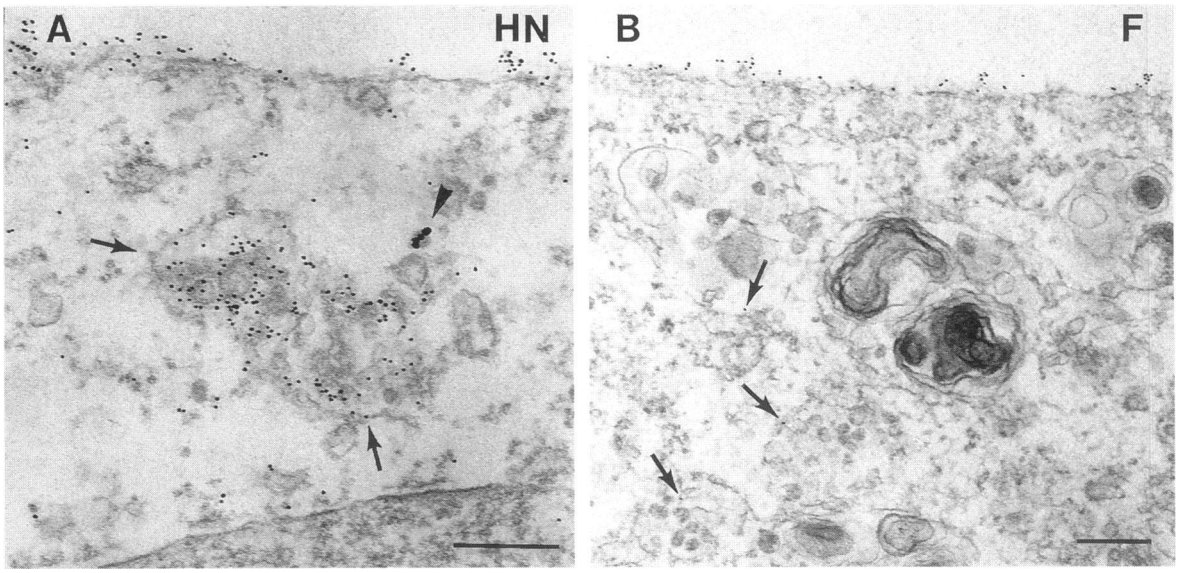

Figure 8. Gold label represents internalized HN. SV5-infected CV-1 cells were incubated in DME minus serum for 30 min at 37°C followed by several washes in DME + 10 mM HEPES, pH 7.4, that had been pre-chilled to 4°C and a 1-h incubation in transferrin coupled to 15 nm gold. Following several washes with DME, cells were flooded with pre-warmed DME + 10 mM HEPES, pH 7.4, containing 100 μg/ml cycloheximide and incubated at 37°C for 90 min. Monolayers were then mildly fixed at room temperature with periodate-lysine-paraformaldehyde, washed with PBS, permeabilized for 15 min in PBS containing 0.1% saponin, and then incubated for 1 h with either mAb HN5a or mAb F1a. Following extensive washing with 0.1% saponin in PBS, antibody binding was visualized by incubating cells for 1 h with secondary antibody coupled to 6 nm gold. Cells were fixed with glutaraldehyde, post-fixed with osmium tetroxide, and processed for EM. Sections were contrasted with uranyl acetate and lead citrate. An endosome (arrows) stained by mAb HN5a is shown in panel A. Transferrin also appears to be associated with this endosome (arrowhead). In comparison, cells stained for the F protein (panel B) showed few gold particles within endosomes (arrows). Bar, 0.25 μm.

arrowhead). Cells stained with the F-specific antibodies shown in Figure 8B demonstrated cell surface staining similar to that observed for HN; however, very little staining of endosomes was found. The few gold particles observed (Figure 8B, arrows) could be the result of trapping of the immunological probes within the cell or may represent a small amount of F that is internalized.

DISCUSSION

The paramyxovirus SV5 HN glycoprotein (565 residues) is a type II orientation integral membrane protein containing a 17-residue cytoplasmic tail, a 19-residue signal-anchor transmembrane domain, and a 529-residue ectodomain that contains four *N*-linked carbohydrate chains (Hiebert *et al.*, 1985; Ng *et al.*, 1989). The HN protein is synthesized in the endoplasmic reticulum, oligomerizes to form a homotetramer, and is transported through the exocytic pathway ($t_{1/2}$ ~75 min to the *medial* Golgi apparatus) where it is abundantly expressed at the plasma membrane (Ng *et al.*, 1989). We have shown previously that HN is internalized from the cell surface (in a manner independent of binding antibody), and degraded ($t_{1/2}$ ~2.5 h) with discrete proteolytic fragments being identifiable (Ng *et al.*, 1989). In comparison, the SV5 F glycoprotein and the hPIV-3 HN protein, which is closely related to SV5 HN, are stably expressed at the plasma membrane.

The HN protein lacks a tyrosine signal in its cytoplasmic tail that is capable of forming a type I β-turn, which is common to many type I and type II orientation receptor proteins, and this signal has been found to be a determinant in the clustering in coated pits and for efficient internalization (Davis *et al.*, 1986; Davis *et al.*, 1987; Lobel *et al.*, 1989; Chen *et al.*, 1990; Jing *et al.*, 1990; McGraw and Maxfield, 1990; McGraw *et al.*, 1991; Lehmann *et al.*, 1992; Thomas and Roth, 1994). Coated pits are estimated to occupy 1–2% of the cell surface and to have a life-time of about 1 min (Anderson *et al.*, 1977a; Griffiths *et al.*, 1989; Pelchen-Matthews *et al.*, 1991; Hansen *et al.*, 1992). The occupancy rate varies widely from 70% of the surface LDL receptors being localized to coated pits (Anderson *et al.*, 1977b), to only 3.5% of the Fc receptor being localized to coated pits (Miettinen *et al.*, 1989). The estimate for the transferrin receptor varies from 6–15% of surface transferrin receptors being associated with clathrin-coated pits (Fuhrer *et al.*, 1991; Miller *et al.*, 1991; Hansen *et al.*, 1992). The magnitude of the effect of removing the tyrosine internalization signal from the

cytoplasmic tail of receptor molecules varies. TfR is internalized efficiently (>90% in 30 min) (Jing *et al.*, 1990). Removal of the cytoplasmic tail of TfR decreases both the rate and total amount of the receptor-ligand complex internalized by >90% (Rothenberger *et al.*, 1987; Iacopetta *et al.*, 1988; Jing *et al.*, 1990; McGraw and Maxfield, 1990). In contrast, the removal of the tyrosine-containing signal from LAP, although not permanently arresting the molecule at the cell surface (mutant LAP was detected in dense lysosomes 2 h after synthesis), changed the rate such that it required about 1 day to deliver one-half of the mutant LAP to lysosomes (Peters *et al.*, 1990). Thus, the mechanism for internalization and delivery of mutant LAP to lysosomes was thought to be by a nonselective stochastic process (Peters *et al.*, 1990) as the $t_{1/2}$ of an average cell surface polypeptide in fibroblasts is 20 h (Draye *et al.*, 1988). Most cell surface proteins that lack tyrosine-containing cytoplasmic tails are thought to turnover at the rate of constitutive membrane turnover. However, a consensus for the rate of basal membrane turnover is lacking as the rate measured ranges from 0.05%/min (or less) to ~2%/min, depending on both the group of investigators and the method of measurement (Steinman *et al.*, 1983; Draye *et al.*, 1988; Davis and Cresswell, 1990; Bretscher, 1992; Almond and Eidels, 1994).

Biochemical analysis to measure the rate of loss of HN protein from the surface of recombinant SV40-infected CV-1 cells showed a $t_{1/2}$ of ~45–50 min for the 60–70% of molecules (Figure 3) that were biotinylated and lost from the cell surface. Although the rate of internalization of HN is slightly slower than that of HA-Y543, a molecule that has been shown to enter CV-1 cells at a rate comparable to cell surface receptors (Lazarovits and Roth, 1988; Ksistakis *et al.*, 1990; Thomas *et al.*, 1993), HN is internalized significantly faster than the rate of basal membrane turnover in CV-1 cells as measured by examining the rate of loss of wt HA from the cell surface (data shown in Figure 3 and Kristakis *et al.*, 1990). It is not known whether the HN molecules that remained at the cell surface formed a stable pool that was resistant to endocytosis or whether the biotinylation procedure caused this effect. The latter explanation is favored as turnover of metabolically labeled HN goes almost to completion in 5 h (Ng *et al.*, 1989). A significant fraction of the biotinylated HN could be recovered inside cells before degradation of HN. Recycling of HN has not been rigorously excluded but overall, internalization of HN appears to be of the nonrecycling type, like epidermal growth factor, tumor necrosis factor, and interleukin 2 receptors (Duprez and Dautry-Varsat, 1986; Watanabe *et al.*, 1988; Felder *et al.*, 1990; Futter *et al.*, 1993), although there is some evidence that suggests that at least a subset of these receptors may be capable of recycling (Masui *et al.*, 1993). Thus, the internalization and degradation rate of HN is significantly faster than a nonselective turn-over of the membrane in CV-1 cells.

Immunocytochemical analysis of gold-labeled viral proteins on the surface of SV5-infected cells showed that HN is internalized via the clathrin-mediated pathway and enters the endosomal system, ultimately localizing to structures with the characteristic morphology of lysosomes. Quantification of gold-labeled HN distribution showed that upon incubation at 37°C, ~5% of the HN on the plasma membrane was localized to coated pits and, after 15 min at 37°C, 88% of the coated pits were labeled. The percent of coated pits containing HN decreased with time of incubation at 37°C as the amount of gold-labeled HN on the cell surface decreased. If 5–6% of HN on the cell surface is localized to coated pits, which have a lifetime of ~1 min, the internalization of HN is at the same rate as the lower estimates of the rate of internalization of TfR. In contrast, for the other SV5 glycoprotein, F protein, only ~0.2% was localized to coated pits but we have not ruled out the possibility that F or hPIV-3 HN is positively excluded from coated pits as is the case for CD4 (Pelchen-Matthews *et al.*, 1991, 1992). Further support for the role of coated pits in HN internalization came from finding that there was a reduction in HN internalization following cytosol acidification, a treatment known to prevent the pinching off of coated pits from the plasma membrane (Sandvig *et al.*, 1987). No labeled HN was found in structures having the morphology of caveolae, and nonselective endocytosis by way of membrane ruffling (Racoosin and Swanson, 1992) was seldom observed and could only account for a small fraction of the total HN gold-label internalized because gold-labeled F protein was predominantly localized to the cell surface.

HN protein could be co-localized with transferrin in coated pits and early endosomes. In early endosomes transferrin releases its iron, and transferrin and its receptor are recycled back to the plasma membrane and are sorted away from the pathway leading to degradation in lysosomes (Eskelinen *et al.*, 1990). However, BSA that is nonselectively pinocytosed and rapidly shuttled to lysosomes (Lippincott-Schwartz and Fambrough, 1987) co-localized with HN in late endocytic/lysosomal compartments. Gold-labeled HN and gold-labeled BSA were found highly aggregated in dense structures having many internal vesicles and membranous structures, the characteristic morphology of late endosomes (van Deurs *et al.*, 1993a).

Thus, the data presented here indicate that internalization of HN occurs via clathrin-coated pits at a rate faster than that of constitutive turnover and HN progresses through endosomal compartments, ultimately becoming localized to lysosomes where pre-

sumably it is degraded. While the cytoplasmic domain of HN does not contain any of the previously identified internalization signals it does contain a transmembrane domain-proximal phenylalanine residue (Hiebert *et al.*, 1985). In the LDL receptor it has been shown (Davis *et al.*, 1987) that phenylalanine, and to a lesser extent tryptophan, can substitute for the critical tyrosine residue for internalization to occur. However, mutagenesis studies indicate the phenylalanine residue in the cytoplasmic domain of HN is not required for internalization (Ector, 1995). Thus, the signal responsible for HN internalization is seemingly not related to those identified to date. Recently, it has been shown that the signal for coated vesicle-mediated internalization of the yeast mating pheromone receptor (Tan *et al.*, 1993), a seven-transmembrane segment polypeptide, is DAKSS, which is contained in the first 39 residues of the receptor cytoplasmic tail (Rohrer *et al.*, 1993). Currently we are making efforts to identify the signal specifying HN-coated pit internalization.

ACKNOWLEDGMENTS

We are very grateful to Michael G. Roth for extensive discussions and for generously providing the SV40 recombinant viruses, wt HA and HA-Y543. We also thank Richard G.W. Anderson, Stuart Kornfeld, Davis T.W. Ng, Sandy L. Schmid, and Angela U. Wandinger-Ness for helpful discussions, Albert I. Farbman for letting us use his microtome, and Gene Minner for maintaining the EM in excellent condition. We also thank Darlene Elia-Buenzow and Craig Anderson for help with confocal microscopy. This work was supported by Research Grant AI-23173 from the National Institute of Allergy and Infectious Diseases. R.A.L. is an Investigator of the Howard Hughes Medical Institute.

REFERENCES

Almond, B.D., and Eidels, L. (1994). The cytoplasmic domain of the Diphtheria toxin receptor (HB-EGF precursor) is not required for receptor-mediated endocytosis. J. Cell Biol. *269*, 26635–26641.

Alvarez, E., Girones, N., and Davis, R.J. (1990). A point mutation in the cytoplasmic domain of the transferrin receptor inhibits endocytosis. Biochem. J. *262*, 31–35.

Anderson, R.G., Brown, M.S., and Goldstein, J.L. (1977a). Role of the coated endocytic vesicle in the uptake of receptor-bound low density lipoprotein in human fibroblasts. Cell *10*, 351–364.

Anderson, R.G.W., Goldstein, J.L., and Brown, M.S. (1977b). A mutation that impairs the ability of lipoprotein receptors to localize in coated pits on the cell surface of human fibroblasts. Nature *270*, 695–699.

Balch, W.E., McCaffery, J.M., Plutner, H., and Farquhar, M.G. (1994). Vesicular stomatitis virus glycoprotein is sorted and concentrated during export from the endoplasmic reticulum. Cell *76*, 841–852.

Bansal, A., and Gierasch, L.M. (1991). The NPXY internalization signal of the LDL receptor adopts a reverse-turn conformation. Cell *67*, 1195–1201.

Bar-Sagi, D., and Feramisco, J.R. (1986). Induction of membrane ruffling and fluid-phase pinocytosis in quiescent fibroblasts by ras proteins. Science *233*, 1061–1068.

Breitfeld, P.P., Casanova, J.E., McKinnon, W.C., and Mostov, K.E. (1990). Deletions in the cytoplasmic domain of the polymeric immunoglobulin receptor differentially affect endocytotic rate and post-endocytotic traffic. J. Biol. Chem. *265*, 13750–13757.

Bretscher, M.S. (1992). Circulating integrins: $\alpha_3\beta_1$, $\alpha_4\beta_1$ or LFA-1. EMBO J. *11*, 405–410.

Chen, W.-J., Goldstein, J.L., and Brown, M.S. (1990). NPXY, a sequence often found in cytoplasmic tails, is required for coated pit-mediated internalization of the low density lipoprotein receptor. J. Biol. Chem. *265*, 3116–3123.

Collawn, J.F., Stangel, M., Kuhn, L., Esekogwu, V., Jing, S., Trowbridge, I.S., and Tainer, J.A. (1990). Transferrin receptor internalization sequence YXRF implicates a tight turn as the structural recognition motif for endocytosis. Cell *63*, 1061–1072.

Davis, C.G., Lehrman, M.A., Russell, D.W., Anderson, R.G.W., Brown, M.S., and Goldstein, J.L. (1986). The J.D. mutation in familial hyper-cholesterolemia: amino acid substitution in cytoplasmic domain impedes internalization of LDL receptors. Cell *45*, 15–24.

Davis, C.G., van Driel, I.R., Russell, D.W., Brown, M.S., and Goldstein, J.L. (1987). The low density lipoprotein receptor. J. Biol. Chem. *262*, 4075–4082.

Davis, J.E., and Cresswell, P. (1990). Lack of detectable endocytosis of B-lymphocyte MHC class II antigens using an antibody-independent technique. J. Immunol. *144*, 990–997.

Doms, R.W., Lamb, R.A., Rose, J.K., and Helenius, A. (1993). Folding and assembly of viral membrane proteins. Virology *193*, 545–562.

Draye, J.P., Courtoy, P.J., Quintart, J., and Baudhuin, P. (1988). A quantitative model of traffic between plasma membrane and secondary lysosomes: evaluation of inflow, lateral diffusion, and degradation. J. Cell Biol. *107*, 2109–2115.

Duprez, V., and Dautry-Varsat, A. (1986). Receptor-mediated endocytosis of interleukin 2 in a human tumor T cell line. J. Biol. Chem. *261*, 15450–15454.

Ector, K.J. (1995). Studies on the internalization of the paramyxovirus SV5 HN glycoprotein. Ph.D. Dissertation. Evanston, IL: Northwestern University.

Eskelinen, S., Kok, J.W., Sormunen, R., and Hoekstra, D. (1990). Coated endosomal vesicles: sorting and recycling compartment for transferrin in BHK cells. Eur. J. Cell Biol. *56*, 210–222.

Felder, S., Miller, K., Moehren, G., Ullrich, A., Schlessinger, J., and Hopkins, C.R. (1990). Kinase activity controls the sorting of the epidermal growth factor receptor within the multivesicular body. Cell *61*, 623–634.

Fuhrer, C., Geffen, I., and Spiess, M. (1991). Endocytosis of the ASGP receptor H1 is reduced by mutation of tyrosine-5 but still occurs via coated pits. J. Cell Biol. *114*, 423–431.

Fujimoto, T. (1993). Calcium pump of the plasma membrane is localized in caveolae. J. Cell Biol. *120*, 1147–1157.

Futter, C.E., Felder, S., Schlessinger, J., Ullrich, A., and Hopkins, C.R. (1993). Annexin I is phosphorylated in the multivesicular body during the processing of the epidermal growth factor receptor. J. Cell Biol. *120*, 77–83.

Ghitescu, L., Fixman, A., Simionescu, M., and Simionescu, N. (1986). Specific binding sites for albumin restricted to plasmalemmal vesicles of continuous capillary endothelium: receptor-mediated transcytosis. J. Cell Biol. *102*, 1304–1311.

Glickman, J.N., Conibear, E., and Pearse, B.M. (1989). Specificity of binding of clathrin adaptors to signals on the mannose-6-phosphate/insulin-like growth factor II receptor. EMBO J. *8*, 1041–1047.

Gorodinsky, A., and Harris, D.A. (1995). Glycolipid-anchored proteins in neuroblastoma cells form detergent-resistant complexes without caveolin. J. Cell Biol. *129*, 619–627.

Griffiths, G., Back, R., and Marsh, M. (1989). A quantitative analysis of the endocytic pathway in baby hamster kidney cells. J. Cell Biol. *109*, 2703–2720.

Hansen, S.H., Sandvig, K., and van Deurs, B. (1992). Internalization efficiency of the transferrin receptor. Exp. Cell Res. *199*, 19–28.

Hiebert, S.W., and Lamb, R.A. (1988). Cell surface expression of glycosylated, nonglycosylated, and truncated forms of a cytoplasmic protein pyruvate kinase. J. Cell Biol. *107*, 865–876.

Hiebert, S.W., Paterson, R.G., and Lamb, R.A. (1985). Hemagglutinin-neuraminidase protein of the paramyxovirus simian virus 5: nucleotide sequence of the mRNA predicts an N-terminal membrane anchor. J. Virol. *54*, 1–6.

Hirsch, J.G., Fedorko, M.E., and Cohn, Z.A. (1968). Vesicle fusion and formation at the surface of pinocytic vacuoles in macrophages. J. Cell Biol. *38*, 629–632.

Hobman, T.C., Woodward, L., and Farquhar, M.G. (1993). The rubella virus E2 and E1 spike glycoproteins are targeted to the Golgi complex. J. Cell Biol. *121*, 269–281.

Hopkins, C.R., and Trowbridge, I.S. (1983). Internalization and processing of transferrin and the transferrin receptor in human carcinoma A431 cells. J. Cell Biol. *97*, 508–521.

Hubbard, A.L. (1989). Endocytosis. Curr. Opin. Cell Biol. *1*, 675–683.

Hunziker, W., Harter, C., Matter, K., and Mellman, I. (1991). Basolateral sorting in MDCK cells requires a distinct cytoplasmic domain determinant. Cell *66*, 907–920.

Iacopetta, B.J., Rothenberger, S., and Kuhn, L.C. (1988). A role for the cytoplasmic domain in transferrin receptor sorting and coated pit formation during endocytosis. Cell *54*, 485–489.

Jing, S., Spencer, T., Miller, K., Hopkins, C., and Trowbridge, I.S. (1990). Role of the human transferrin receptor cytoplasmic domain in endocytosis: localization of a specific signal sequence for internalization. J. Cell Biol. *110*, 283–294.

Keller, G.-A., Siegel, M.W., and Caras, I.W. (1992). Endocytosis of glycolipid-anchored and transmembrane forms of CD4 by different endocytic pathways. EMBO J. *11*, 863–874.

Krijnse-Locker, J., Ericsson, M., Rottier, P.J.M., and Griffiths, G. (1994). Characterization of the budding compartment of mouse hepatitis virus: evidence that transport from the RER to the Golgi complex requires only one vesicular transport step. J. Cell Biol. *124*, 55–70.

Ktistakis, N.T., Thomas, D., and Roth, M.G. (1990). Characteristics of the tyrosine recognition signal for internalization of transmembrane surface glycoproteins. J. Cell Biol. *111*, 1393–1407.

Lazarovits, J., and Roth, M. (1988). A single amino acid change in the cytoplasmic domain allows the influenza virus hemagglutinin to be endocytosed through coated pits. Cell *53*, 743–752.

Le Bivic, A., Real, F.X., and Rodriguez-Boulan, E. (1989). Vectorial targeting of apical and basolateral plasma membrane proteins in a human adenocarcinoma epithelial cell line. Proc. Natl. Acad. Sci. USA *86*, 9313–9317.

Lehmann, L.E., Eberle, W., Krull, S., Prill, V., Schmidt, B., Sander, C., von Figura, K., and Peters, C. (1992). The internalization signal in the cytoplasmic tail of lysosomal acid phosphatase consists of the hexapeptide PGYRHV. EMBO J. *11*, 4391–4399.

Lehrman, M.A., Goldstein, J.L., Brown, M.S., Russell, D.W., and Schneider, W.J. (1985). Internalization-defective LDL receptors by genes with non-sense and frameshift mutations that truncate the cytoplasmic domain. Cell *41*, 735–743.

Lippincott-Schwartz, J., and Fambrough, D.M. (1987). Cycling of the integral membrane glycoprotein, LEP100, between plasma membrane and lysosomes: kinetic and morphological analysis. Cell *49*, 669–677.

Lobel, P., Fujimoto, K., Ye, R.D., Griffiths, G., and Kornfeld, S. (1989). Mutations in the cytoplasmic domain of the 275 kd mannose 6-phosphate receptor differentially alter lysosomal enzyme sorting and endocytosis. Cell *57*, 787–796.

Masui, H., Castro, L., and Mendelsohn, J. (1993). Consumption of EGF by A431 cells: evidence for receptor recycling. J. Cell Biol. *120*, 85–93.

Matlin, K., Bainton, D.F., Pesonen, M., Louvard, D., Genty, N., and Simons, K. (1983). Transepithelial transport of a viral membrane glycoprotein implanted into the apical plasma membrane of Madin-Darby canine kidney cells. I. Morphological evidence. J. Cell Biol. *97*, 627–637.

McGraw, T.E., and Maxfield, F.R. (1990). Human transferrin receptor internalization is partially dependent upon an aromatic amino acid on the cytoplasmic tail. Cell Regul. *1*, 369–377.

McGraw, T.E., Pytowski, B., Arzt, J., and Ferrone, C. (1991). Mutagenesis of the human transferrin receptor: two cytoplasmic phenylalanines are required for efficient internalization and a second-site mutation is capable of reverting an internalization-defective phenotype. J. Cell Biol. *112*, 853–861.

McLean, I.W., and Nakane, P.K. (1974). Periodate-lysine-paraformaldehyde: a new fixative for immunoelectron microscopy. J. Histochem. Cytochem. *22*, 1077–1083.

Miettinen, H.M., Rose, J.K., and Mellman, I. (1989). Fc receptor isoforms exhibit distinct abilities for coated pit localization as a result of cytoplasmic domain heterogeneity. Cell *58*, 317–327.

Miller, K., Shipman, M., Trowbridge, I.S., and Hopkins, C.R. (1991). Transferrin receptors promote the formation of clathrin lattices. Cell *65*, 621–632.

Montesano, R., Roth, J., Robert, A., and Orci, L. (1982). Non-coated membrane invaginations are involved in binding and internalization of cholera and tetanus toxins. Nature *296*, 651–653.

Neutra, M.R., Ciechanover, A., Owen, L.S., and Lodish, H.F. (1985). Intracellular transport of transferrin- and asialoorosomucoid-colloidal gold conjugated to lysosomes after receptor-mediated endocytosis. J. Histochem. Cytochem. *33*, 1134–1144.

Ng, D.T.W., Randall, R.E., and Lamb, R.A. (1989). Intracellular maturation and transport of the SV5 type II glycoprotein hemagglutinin-neuraminidase: specific and transient association with GRP78-BiP in the endoplasmic reticulum and extensive internalization from the cell surface. J. Cell Biol. *109*, 3273–3289.

Parton, R.G., Joggerst, B., and Simons, K. (1994). Regulated internalization of caveolae. J. Cell Biol. *127*, 1199–1215.

Paterson, R.G., Harris, T.J.R., and Lamb, R.A. (1984). Fusion protein of the paramyxovirus simian virus 5: nucleotide sequence of mRNA predicts a highly hydrophobic glycoprotein. Proc. Natl. Acad. Sci. USA *81*, 6706–6710.

Pearse, B.M.F. (1988). Receptors compete for adaptors found in plasma membrane-coated pits. EMBO J. *7*, 3331–3336.

Pelchen-Matthews, A., Armes, J.E., Griffiths, G., and Marsh, M. (1991). Differential endocytosis of CD4 in lymphocytic and nonlymphocytic cells. J. Exp. Med. *173*, 575–587.

Pelchen-Matthews, A., Boulet, I., Littman, D.R., Fagard, R., and Marsh, M. (1992). The protein tyrosine kinase $p56^{lck}$ inhibits CD4 endocytosis by preventing entry of CD4 into coated pits. J. Cell Biol. *117*, 279–290.

Peters, C., Braun, M., Weber, B., Wendland, M., Schmidt, B., Pohlmann, R., Waheed, A., and von Figura, K. (1990). Targeting of a lysosomal membrane protein: a tyrosine-containing endocytosis sig-

nal in the cytoplasmic tail of lysosomal acid phosphatase is necessary and sufficient for targeting to lysosomes. EMBO J. *9*, 3497–3506.

Racoosin, E.L., and Swanson, J.A. (1992). M-CSF-induced macropinocytosis increases solute endocytosis but not receptor-mediated endocytosis in mouse macrophages. J. Cell Sci. *102*, 867–880.

Randall, R.E., Young, D.F., Goswami, K.K.A., and Russell, W.C. (1987). Isolation and characterization of monoclonal antibodies to simian virus 5 and their use in revealing antigenic differences between human, canine and simian isolates. J. Gen. Virol. *68*, 2769–2780.

Roettger, B.F., Rentsch, R.U., Pinon, D., Holicky, E., Larkin, J.M., and Miller, L.J. (1995). Dual pathways of internalization of the cholecystokinin receptor. J. Cell Biol. *128*, 1029–1041.

Rohrer, J., Benedetti, H., Zanolari, B., and Riezman, H. (1993). Identification of a novel sequence mediating regulated endocytosis of the G protein-coupled α-pheromone receptor in yeast. Mol. Biol. Cell *4*, 511–521.

Roth, M.G., Doyle, C., Sambrook, J., and Gething, M.-J. (1986). Heterologous transmembrane and cytoplasmic domains direct functional chimeric influenza virus hemagglutinins into the endocytic pathway. J. Cell Biol. *102*, 1271–1283.

Rothberg, K.G., Ying, Y., Kolhouse, J.F., Kamen, B.A., and Anderson, R.G.W. (1990). The glycophospholipid-linked folate receptor internalizes folate without entering the clathrin-coated pit endocytic pathway. J. Cell Biol. *110*, 637–649.

Rothenberger, S., Iacopetta, B.J., and Kuhn, L.C. (1987). Endocytosis of the transferrin receptor requires the cytoplasmic domain but not its phosphorylation site. Cell *49*, 423–431.

Sandvig, K., Olsnes, S., Petersen, S.O., and van Deurs, B. (1987). Acidification of the cytosol inhibits endocytosis from coated pits. J. Cell Biol. *105*, 679–689.

Scherer, P.E., Lisanti, M.P., Baldini, G., Sargiacomo, M., Mastick, C.C., and Lodish, H.F. (1994). Induction of caveolin during adipogenesis and association of GLUT4 with caveolin-rich vesicles. J. Cell Biol. *127*, 1233–1243.

Schmid, S.L., and Smythe, E. (1991). Stage-specific assays for coated pit formation and coated vesicle budding in vitro. J. Cell Biol. *114*, 869–880.

Shyng, S.-L., Heuser, J.E., and Harris, D.A. (1994). A glycolipid-anchored prion protein is endocytosed via clathrin-coated pits. J. Cell Biol. *125*, 1239–1250.

Slot, J.W., and Geuze, H.J. (1985). A new method for preparing gold probes for multiple-labeling cytochemistry. Eur. J. Cell Biol. *38*, 87–93.

Smythe, E., Carter, L.L., and Schmid, S.L. (1992). Cytosol- and clathrin-dependent stimulation of endocytosis in vitro by purified adaptors. J. Cell Biol. *119*, 1163–1171.

Steinman, R.M., Mellman, I.S., Muller, W.A., and Cohn, Z.A. (1983). Endocytosis and the recycling of plasma membrane. J. Cell Biol. *96*, 1–27.

Tan, P.K., Davis, N.G., Sprague, G.F., and Payne, G.S. (1993). Clathrin facilitates the internalization of seven transmembrane segment receptors for mating pheromones in yeast. J. Cell Biol. *123*, 1707–1716.

Thomas, D.C., Brewer, C.B., and Roth, M.G. (1993). Vesicular stomatitis virus glycoprotein contains a dominant cytoplasmic basolateral sorting signal critically dependent upon a tyrosine. J. Biol. Chem. *268*, 3313–3320.

Thomas, D.C., and Roth, M.G. (1994). The basolateral targeting signal in the cytoplasmic domain of glycoprotein G from vesicular stomatitis virus resembles a variety of intracellular targeting motifs related by primary sequence but having diverse targeting activities. J. Biol. Chem. *269*, 15732–15739.

Trowbridge, I.S., Collawn, J.F., and Hopkins, C.R. (1993). Signal-dependent membrane protein trafficking in the endocytic pathway. Annu. Rev. Cell Biol. *9*, 129–161.

van Deurs, B., Holm, P.K., Kayser, L., Sandvig, K., and Hansen, S.H. (1993a). Multivesicular bodies in HEp-2 cells are maturing endosomes. Eur. J. Cell Biol. *61*, 208–224.

van Deurs, B., Holm, P.K., Sandvig, K., and Hansen, S.H. (1993b). Are caveolae involved in clathrin-independent endocytosis? Trends Cell Biol. *3*, 249–251.

van Wyke-Coelingh, K., and Tierney, E.L. (1989). Antigenic and functional organization of human parainfluenza virus type 3 fusion glycoprotein. J. Virol. *63*, 375–382.

Watanabe, N., Kuriyama, H., Sone, H., Yamauchi, N., Maeda, M., and Niitsu, Y. (1988). Continuous internalization of tumor necrosis factor in a human myosarcoma cell line. J. Biol. Chem. *263*, 10262–10266.

Watts, C., and Marsh, M. (1992). Endocytosis: what goes in and how? J. Cell Sci. *103*, 1–8.

Weibel, E.R. (1979). Stereological Methods: Practical Methods for Biological Morphometry, London, United Kingdom: Academic Press.

West, M.A., Bretscher, M.S., and Watts, C. (1989). Distinct endocytic pathways in epidermal growth factor-stimulated human carcinoma A431 cells. J. Cell Biol. *109*, 2731–2739.

Woods, J.W., Goodhouse, J., and Farquhar, M.G. (1989). Transferrin receptors and cation-independent mannose-6-phosphate receptors deliver their ligands to two distinct subpopulations of multivesicular endosomes. Eur. J. Cell Biol. *50*, 132–143.